COLLEGE of CHARLESTON

MATH 645

Numerical Analysis II

Professor: Dr. Daniel Poll

[redacted]

Fall 2021

Contents

1 Introduction

Diffusion processes occur in many contexts. Expansion of urban areas into the suburbs and beyond, dispersion of a dye or chemical in a container of water, the heating of a steel plate, or growth of a biofilm are just a few examples. However, in most real-world contexts, there are other interactions that are also occuring. Growth of a biofilm is affected by the amount of food available, the specific (local) non-homogeneity of the steel affects the rate of energy transfer, chemical reactions can occur and change the concentration of the additive, and geographical features and traffic constraints modify housing development. Thus a more complete model of any of these processes is the Reaction-Diffusion model. Additionally, due to the quantized nature of molecules of a chemical, the atoms of elements in steel, or the single organisms in a biofilm or house, there is also a stochasitic effect that can be discussed.

In this paper, we will be modeling the dynamics of a predator-prey interaction with the Holling type II functional response and logistic growth of the prey using a finite-difference algorithm[1]. This algorithm is stable and convergent with a small enough time step, which is very useful since approximating differential equations can produce results that differ significantly from analyzing the differential equations themselves. Also, this allows us to use standard direct and iterative solvers, and guarantee their convergence, since the resulting system of equations will be linear. Finally, we will discuss the stochastic effects on our numerical results, although we will not be simulating them. For a more in-depth discussion of the stochastics, see Liu, et al[2].

Rather than duplicating much of Garvie's work, we will simply quote his results and accept them as fact. Our primary focus is on the numerical simulation, not the underlying mathematical rigor. As such, much of the material in this section is essentially quoted from [1], although edited for brevity.

1.1 Model Equations

The general form for our predator-prey reaction-diffusion system is

$$\begin{cases} \dfrac{\partial u}{\partial t} = \delta_1 \Delta u + r\, u \left(1 - \dfrac{u}{w}\right) - p\, v\, h(ku) \\ \dfrac{\partial v}{\partial t} = \delta_2 \Delta v + q\, v\, h(ku) - s\, v \end{cases} \tag{1}$$

where $u(\vec{x},t)$ and $v(\vec{x},t)$ are the population densities of prey and predator at time t and vector position $\vec{x}$, Δ is the LaPlacian operator, and the parameters δ_1, δ_2, r, w, p, k, q, and s are strictly positive. Finally, the *functional response* $h(\cdot)$ is assumed to be a C^2 function with the following conditions:

1. $h(0) = 0$,

2. $\lim_{x\to\infty} h(x) = 1$,
3. $h(\cdot)$ is strictly increasing on $[0,\infty)$.

The positive parameters relate the various aspects of the predators and prey to themselves and to each other. First, the functional response h represents prey consumption rate as a fraction of maximum rate, p. The constant k determines the rate at which consumption rate saturates as prey population increases. Maximum per capita birth rates are q (predator) and r (prey) and death rate of predator is s. Finally, w is the prey-carrying capacity. Once again, the growth rate of the prey is logistic, and the predator shows the Holling Type II functional response. As mentioned previously, this model describes the effect of predators on a prey population, but specifically does not include stochastic effects or the environment.

In order to simplify the calculations involved and specifically the number of parameters, we will rescale Equation 1 to a non-dimensional form. Our substitutions are

$$\tilde{u} = \frac{u}{w} \qquad \tilde{v} = v\left(\frac{p}{r\,w}\right) \qquad \tilde{t} = r\,t \qquad \tilde{x_i} = x_i\left(\frac{r}{\delta_1}\right)^{1/2}$$

and the parameters rescale to

$$a = k\,w \qquad b = \frac{q}{r} \qquad c = \frac{s}{r} \qquad \delta = \frac{\delta_1}{\delta_2}$$

Thus we will simulate the following non-dimensional system

$$\begin{cases} \dfrac{\partial u}{\partial t} = \Delta u + u\,(1-u) - v\,h(au) = \Delta u + f(u,v) \\ \dfrac{\partial v}{\partial t} = \delta\Delta v + b\,v\,h(au) - c\,v = \delta\Delta v + g(u,v) \end{cases} \tag{2}$$

with strictly positive parameters a, b, c, and δ. Additionally, we will assume the system is defined on a bounded domain Ω (the habitat) and we will specify appropriate initial and boundary conditions. Since we will assume that neither the predators nor the prey leave the domain, we will use homogeneous Neumann (or zero-flux) boundary conditions.

Garvie presents two different functional responses affecting the non-linear portion of our model, and also two different numerical schemes. Both schemes are semi-implicit (in time) and produce nearly the same results for relatively short time horizons, but rather different long-time results. Garvie suggests at least two possible reasons for this. However, we will only use one scheme, as we desire to compare the two different functional responses.

As Garvie, we will use previous research[1] and focus on two specific type II functional responses with positive parameters α, β, and γ

$$h(\eta) = h_1(\eta) = \frac{\eta}{1+\eta} \qquad (\eta = au), \qquad \text{with } a = \frac{1}{\alpha},\ b = \beta,\ c = \gamma \tag{3a}$$

$$h(\eta) = h_2(\eta) = 1 - e^{-\eta} \qquad (\eta = au), \qquad \text{with } a = \gamma,\ c = \beta,\ b = \alpha\beta \tag{3b}$$

Substituting these into Equation 2 gives us the following two pairs of kinetics functions.

$$\begin{cases} f_1(u,v) = u(1-u) - \dfrac{uv}{u+\alpha} \\ g_1(u,v) = \dfrac{\beta uv}{u+\alpha} - \gamma v \end{cases} \tag{4a}$$

$$\begin{cases} f_2(u,v) = u(1-u) - v\left(1 - e^{-\gamma u}\right) \\ g_2(u,v) = \beta v\left(\alpha - 1 - \alpha e^{-\gamma u}\right) \end{cases} \tag{4b}$$

Our choice of parameters must consider the local dynamics of the system, and naturally, we must assume $u \geq 0$ and $v \geq 0$. Also, there is a stationary point (u^*, v^*) (that is, $f = g = 0$) corresponding to the coexistence of prey and predators, which we can find as

$$\begin{cases} u_1^* = \dfrac{\alpha\gamma}{\beta - \gamma} \\ v_1^* = (1-u^*)(u^*+\alpha) \end{cases} \qquad \text{with } \beta > \gamma,\ \alpha < \frac{\beta-\gamma}{\gamma}$$

$$\begin{cases} u_2^* = -\dfrac{1}{\gamma}\ln\left(\dfrac{\alpha-1}{\alpha}\right) \\ v_2^* = \dfrac{u^*(1-u^*)}{1-e^{-\gamma u^*}} \end{cases} \qquad \text{with } \alpha > 1,\ \gamma > -\ln\left(\frac{\alpha-1}{\alpha}\right)$$

for the two kinetics equations (4a & 4b) respectively. Note this also requires $0 < u^* < 1$ and that the growth rate of the predator must exceed its death rate ($b > c$). Including stochastic effects, however, can result in extinction of the predator and/or prey.[2]

The rest of this paper is organized as follows. In Section 2 we discuss the finite-difference scheme we use to approximate the solutions of Equation 2 in two spatial dimensions. In Section 3 we present our results, with the Python script attached in Appendix C. In Section 4 we make some concluding comments, including a comparison to Garvie's original results in [1].

2 Numerical Solution of the Model Equations

2.1 Motivation

We desire to compare the results of the two different functional responses for similar initial conditions to determine the effect (if any) of our assumptions about the way predators and prey interact. That is, is there a significant difference in the results from the two different Type II functional responses. Since realistic models (like ours) are nonlinear, we need to use numerical methods[1]. Additionally, we will use finite-difference and finite-element methods for the same reasons as Garvie.

2.2 Preliminaries

We will be performing this comparison in two dimensions, so we will uniformly divide the square $\Omega = [A,B] \times [A,B]$ using a spatial step size h. Thus our grid points will be $(x_i, y_j) = (ih + A, jh + A)$ with $i, j = 0, \ldots, M$ and $M = (B - A)/h$. For simplicity, we will assume the lower left-hand corner of our domain is the origin, so $(x_0, y_0) = (A, A) = (0, 0)$ and $B = Mh$. Thus $(x_i, y_j) = (i, j)$. Time will also be uniformly discretized on the interval $[0, T]$ and $t_k = k\Delta t$ with $k = 0, \ldots, N$ and $T/N = \Delta t$. Again for simplicity we will use $T = 1$ and so $\Delta t = 1/N$ where N is the number of time steps we want to simulate. This is consistent with our non-dimensionalization of the original model. Similar to Garvie, we will use $\vec{\Phi}^k_{i,j} = (U^k_{i,j}, V^k_{i,j})$ is the approximation of $\vec{\phi}(x_i, y_j, t_k) = (u(x_i, y_j, t_k), v(x_i, y_j, t_k))$. The implementation of our algorithm will require vectorizing (in space) so we will use the so-called "natural numbering" used by Garvie, and so for each time step, $U_{i,j} = U_p$ and $V_{i,j} = V_p$ where $p = i + j(M + 1)$ and so $p = 0, \ldots, (M + 1)^2 = P$.

In order to maintain stability in our finite-difference methods, we will modify the functional responses (Equations 3a and 3b) to

$$\widehat{h_1}(\chi) = \frac{\chi}{1 + |\chi|} \tag{5}$$

$$\widehat{h_2}(\chi) = 1 - e^{-|\chi|} \tag{6}$$

which then modifies the logistic growth term (of the prey) to

$$\chi(1 - \chi) \longrightarrow \chi(1 - |\chi|)$$

2.3 General Form of the Difference Scheme

Similar to the functional responses, we will denote the modified discrete kinetic functions as $\widehat{f}$ and $\widehat{g}$. Then our linear scheme has the following general form.

For $k = 1, \ldots, N$ and $i, j = 0, \ldots, M$, find $\{U_{i,j}^k, V_{i,j}^k\}$ such that

$$\begin{cases} \partial_k U_{i,j}^k = \Delta_h U_{i,j}^k + \widehat{f}(\vec{\Phi}_{i,j}^k, \vec{\Phi}_{i,j}^{k-1}) \\ \partial_k V_{i,j}^k = \delta \Delta_h V_{i,j}^k + \widehat{g}(\vec{\Phi}_{i,j}^k, \vec{\Phi}_{i,j}^{k-1}) \end{cases} \tag{7}$$

with an initial approximation of

$$U_{i,j}^0 := u_0(x_i, y_j) \qquad\qquad V_{i,j}^0 := v_0(x_i, y_j) \tag{8}$$

We also need several equations to approximate the zero-flux boundary conditions. These are attached in Appendix A.

2.4 Numerical Scheme

Our numerical scheme involves an approximation of the reaction kinetics using terms from both the previous and the current time step. Since we are trying to solve for the current time step, this is an implicit (in time) numerical scheme. The kinetics of 7 for functional response 5 are

$$\widehat{f}(\vec{\Phi}_{i,j}^k, \vec{\Phi}_{i,j}^{k-1}) = f_1(\vec{\Phi}_{i,j}^k, \vec{\Phi}_{i,j}^{k-1}) = U_{i,j}^k - U_{i,j}^k \left| U_{i,j}^{k-1} \right| - V_{i,j}^k \widehat{h_1}(a U_{i,j}^{k-1}) \tag{9a}$$

$$= U_{i,j}^k - U_{i,j}^k \left| U_{i,j}^{k-1} \right| - V_{i,j}^k \left(\frac{a U_{i,j}^{k-1}}{1 + \left| a U_{i,j}^{k-1} \right|} \right)$$

$$\widehat{g}(\vec{\Phi}_{i,j}^k, \vec{\Phi}_{i,j}^{k-1}) = g_1(\vec{\Phi}_{i,j}^k, \vec{\Phi}_{i,j}^{k-1}) = b V_{i,j}^k \widehat{h_1}(a U_{i,j}^{k-1}) - c V_{i,j}^k \tag{9b}$$

$$= b V_{i,j}^k \left(\frac{a U_{i,j}^{k-1}}{1 + \left| a U_{i,j}^{k-1} \right|} \right) - c V_{i,j}^k$$

and the kinetics for functional response 6 are

$$\widehat{f}(\vec{\Phi}_{i,j}^{k},\vec{\Phi}_{i,j}^{k-1}) = f_2(\vec{\Phi}_{i,j}^{k},\vec{\Phi}_{i,j}^{k-1}) = U_{i,j}^{k} - U_{i,j}^{k}\left|U_{i,j}^{k-1}\right| - V_{i,j}^{k}\widehat{h_2}(aU_{i,j}^{k-1}) \tag{10a}$$

$$= U_{i,j}^{k} - U_{i,j}^{k}\left|U_{i,j}^{k-1}\right| - V_{i,j}^{k}\left(1 - e^{-\left|aU_{i,j}^{k-1}\right|}\right)$$

$$\widehat{g}(\vec{\Phi}_{i,j}^{k},\vec{\Phi}_{i,j}^{k-1}) = g_2(\vec{\Phi}_{i,j}^{k},\vec{\Phi}_{i,j}^{k-1}) = bV_{i,j}^{k}\widehat{h_2}(aU_{i,j}^{k-1}) - cV_{i,j}^{k} \tag{10b}$$

$$= bV_{i,j}^{k}\left(1 - e^{-\left|aU_{i,j}^{k-1}\right|}\right) - cV_{i,j}^{k}$$

We can simplify both of these to the same block matrix equation

$$\begin{bmatrix} A^{k-1} & B^{k-1} \\ 0 & C^{k-1} \end{bmatrix}\begin{bmatrix} \vec{U}^{k} \\ \vec{V}^{k} \end{bmatrix} = \begin{bmatrix} \vec{U}^{k-1} \\ \vec{V}^{k-1} \end{bmatrix} \qquad 1 \le k \le N \tag{11}$$

where

$$\vec{U}^{k} = (U_0^{k},\ldots,U_P^{k})^{T} \qquad \vec{V}^{k} = (V_0^{k},\ldots,V_P^{k})^{T}$$

The coefficient matrices A, B, and C (which depend on the solution at time t_{k-1}) and the associated constant coefficient matrix are given in Appendix B.

2.5 Algorithms

At each time step, we will need two stages in order to solve Equation 11. First, we will get an approximate solution for Φ using a Gauss-Seidel iteration. Then we will use that as part of a SOR iteration. At each time step, we will consider convergence to be a low residual while limiting the total number of SOR iterations. We have seen that SOR converges to the unique solution of $A\vec{x} = \vec{b}$ for any initial approximation if A is diagonally dominant, which is true for our coefficient matrix.

3 Results

Figure 1 shows the initial distribution of predators and prey and the following figures show the two different functional responses and successive refinement of Δt. For all of these figures, the left image is the distribution of predators and the right image is the distribution of prey. As Garvie used very different initial conditions for the second functional response (3b), no direct comparison to his results can be made. However, we will compare our results for Functional Response 3a to his, and then our results for both Functional Responses to each other.

A comparison of Figures 2 and 3 shows results that pretty closely match Garvie's. Interestingly, our spiral turns the opposite direction from his, although that may be an artifact of the method of reshaping the initial data grid to the initial solution vector and the final solution vector back to a grid for plotting. Additionally, the prey are more spread out than the predators, which is a reasonable expectation. Finally note, as expected, a refinement in Δt from $1/3$ to $1/24$ results in a more open spiral.

On the other hand, the two functional responses produced very different results. Using Garvie's initial conditions we duplicate his results, as expected. However, using our initial conditions instead seems to give us approximately oscillatory results which is something we would expect from more stochastic effects[2]. These results seem rather odd on the surface.

If we had not obtained Garvie's results from his initial conditions for Functional Response 2, we would suspect something wrong in our simulation. However, it appears our entering assumption that the two functional responses are independent of intial predator and prey distributions is faulty. That is, it seems the exponential functional response 3b is an initial result of the invasion of prey by predators, and after some length of time, the less uniform distribution of predators and prey results in the rational functional response 3a.

To verify our hypothesis regarding long-term interaction between predator and prey, we ran a (single) long-time-scale simulation of invasion by predators into a uniform distribution of prey. Our initial conditions (which mimic Garvie's) and results for the two functional responses are shown in Figure 7 below. The circular pattern in these results is clearly an artifact of the initial conditions. However, the semi-random scattering patterns are very similar to the results of the long-time-scale simulation for our initial conditions, shown in Figure 4. Note: In Figure 7 the plots are Top: Initial Conditions; Middle: Functional Response 3a; Bottom: Functional Response 3b.

$$U^0_{i,j} = u^* - 2 \times 10^{-7}(x_i - 0.1y_j - 225)(x_i - 0.1y_j - 675)$$

$$V^0_{i,j} = v^* - 3 \times 10^{-5}(x_i - 450) - 1.2 \times 10^{-4}(y_j - 150)$$

Table 1: Initial Conditions for All Simulations except Figure 7

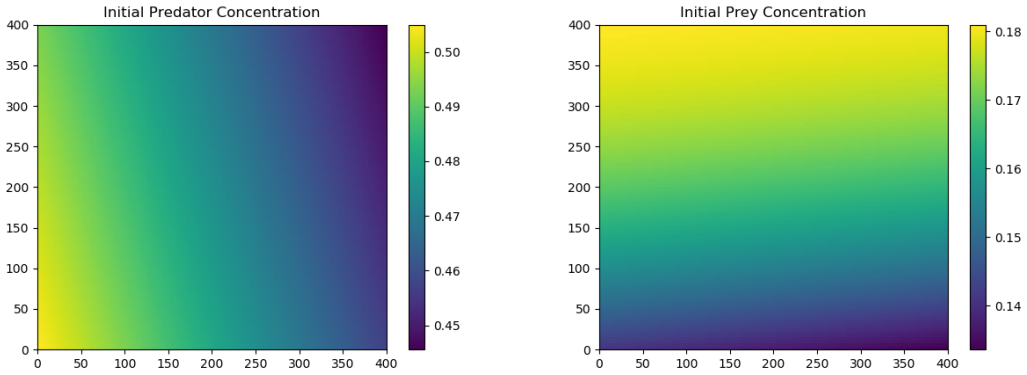

Figure 1: Initial Conditions for Figures 2-6

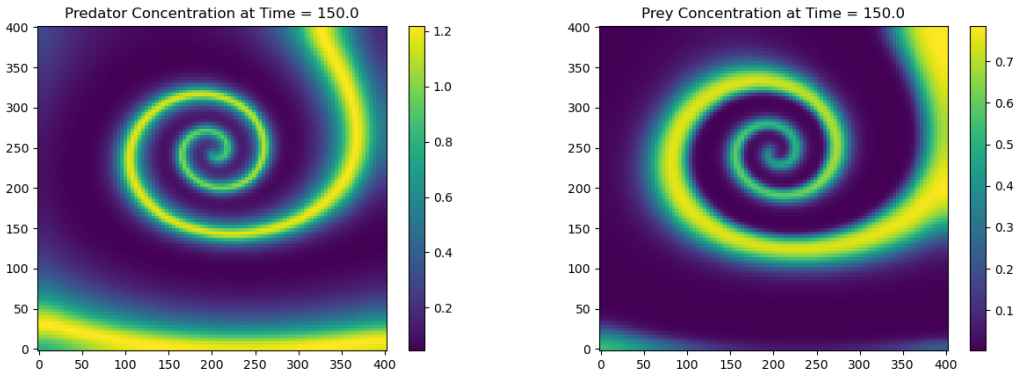

Figure 2: Results for Functional Response 1 and $\Delta t = \frac{1}{3}$

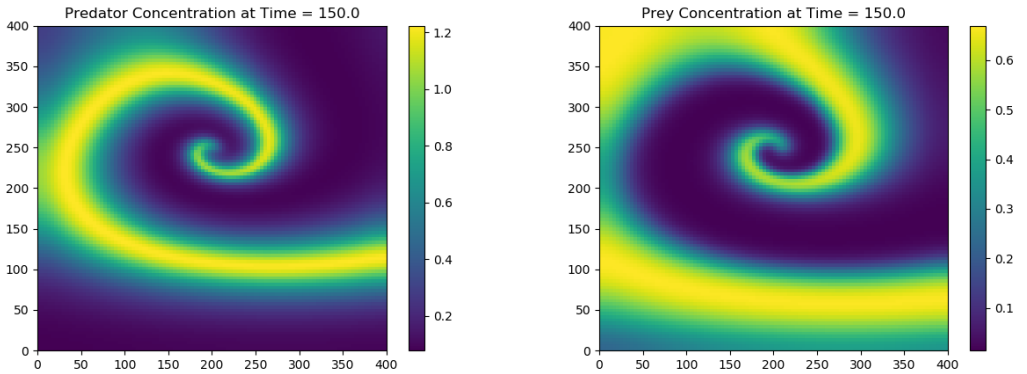

Figure 3: Results for Functional Response 1 and $\Delta t = \frac{1}{24}$

The parameter values used for the two different functional responses are tabulated in Table 3 and the intial conditions are specified in Table 1. These parameter values and initial conditions mimic those of Garvie[1].

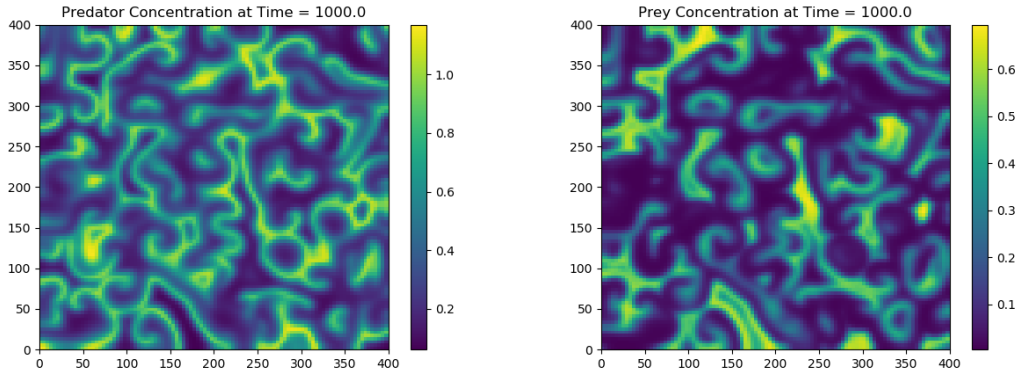

Figure 4: Results for Functional Response 1 and $\Delta t = \frac{1}{3}$ (Long-Time)

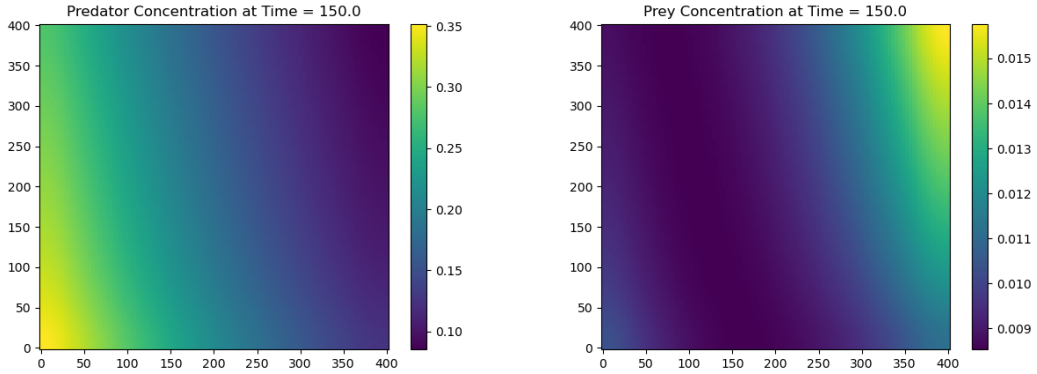

Figure 5: Results for Functional Response 2 and $\Delta t = \frac{1}{3}$

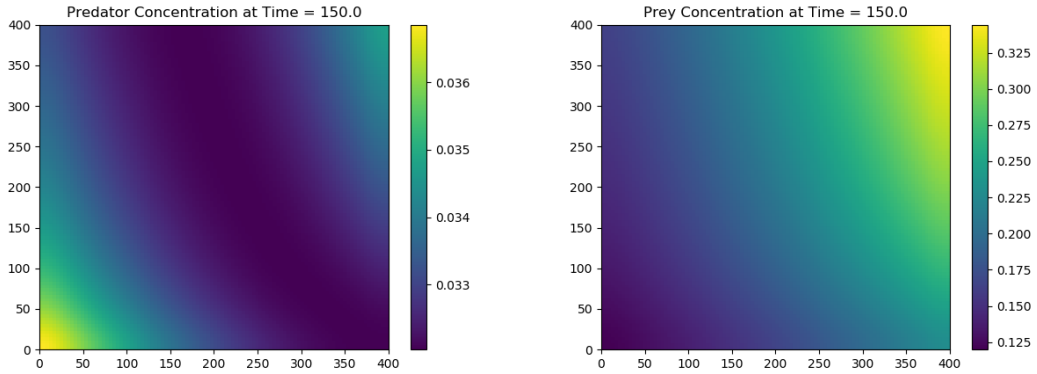

Figure 6: Results for Functional Response 2 and $\Delta t = \frac{1}{24}$

Finally, we present a simulation of Functional Response 3b on a large, 1000×1000, spatial region (Figure 8) rather than the 400×400 region that is the focus of our comparison between functional responses. Although only a single data point, we feel this result

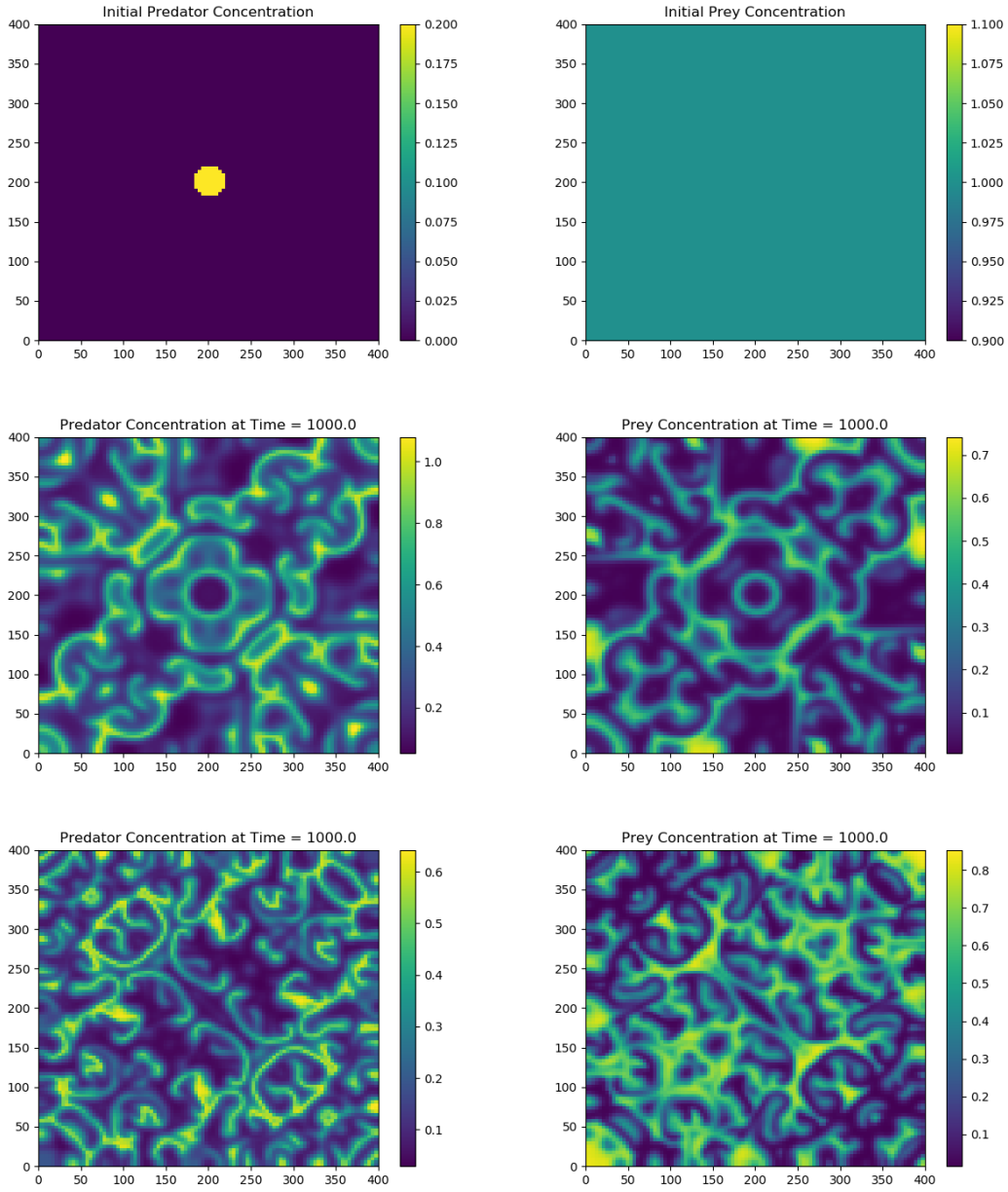

Figure 7: Results for Both Functional Responses and $\Delta t = \frac{1}{3}$ (Long-Time)

$$U^0_{i,j} = 1$$

$$V^0_{i,j} = \begin{cases} 0.2 & x_i^2 + y_j^2 \leq 400 \\ 0.0 & \text{else} \end{cases}$$

Table 2: Initial Conditions for Figure 7

validates Garvie's results that the domain does not seem to significantly affect results for

the same boundary conditions.

Parameter	**Value ($\hat{h_1}$)**	**Value ($\hat{h_2}$)**
α	0.4	1.5
β	2.0	1.0
γ	0.6	5.0
δ	1.0	1.0
u^*	6/35	6/35
v^*	116/245	116/245

Table 3: Parameter Values for Functional Responses $\widehat{h_1}$ and $\widehat{h_2}$

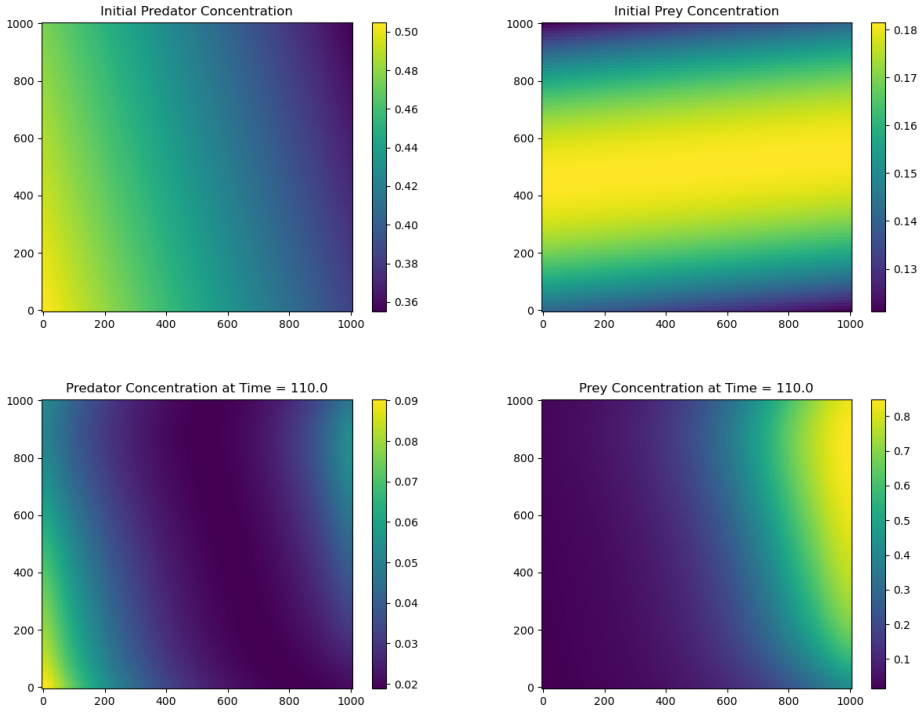

Figure 8: Results for Functional Response 2 and $\Delta t = \frac{1}{3}$ on Large Area

4 Concluding Remarks

The two functional responses produced vastly different results for similar initial conditions. At this time, we believe the differences should be attributed to the difference in long-time predator/prey interaction represented by Functional Response 3a and the initial prey invasion by a predator interaction represented by Functional Response 3b. That is, initial invasion results in a higher consumption of prey by the predator. After the predator and prey have dispersed, the consumption rate lowers and oscillatory behavior begins as stochastic effects take over, as described in [2].

4.1 Stochastic Effects

Although not the primary focus of this paper, stochastic effects present some additional points for discussion. These effects produce one of two results. Either the predator and prey die out, or the concentrations of predator and prey species oscillate around some average value. The rest of this section is primarily comments on a paper by Liu, et al[2].

Aside from the lack of stochastics in our model, there are two other primary differences to be addressed to compare the two models. First, Liu uses a coupled triplet of Ordinary Differential Equations, where the dependent variables are densities as a function of only time rather than both location and time. Thus there is no diffusion term, as there is nowhere for the species to diffuse to or from. Second, they use a "stage structure" splitting the predators into "immature" and "mature" stages rather than the somewhat more simple predator-prey structure we have used. Thus the prey is only affected by the mature predator density.

These two differences make direct comparison between our results and theirs somewhat difficult. However, we will attempt to make a few statements that relate the two sets of results and point out some ideas that we find interesting and suggest why a closer comparison could be valuable.

4.1.1 Extinction

Extinction occurs due either to direct effects (e.g., over-hunting) or indirect effects (e.g., destruction of habitat). If the prey becomes extinct, the predator soon follows, but the predator can become extinct even if the prey survives. In the referenced paper, Liu determines the sufficient conditions on prey growth rates and predator maturation/death rates to cause extinction of the predator in both cases. Of note is the inclusion of stochastic effects (via Brownian motion) of the non-continuous nature of real animals in the wild.

4.1.2 Oscillation

Although Liu focuses on the extinction of the predator, non-extinction numerical results are presented first. That is, an ergodic stationary distribution of the stochastic system of differential equations exists. This system of equations simply adds a term to each equation in 1 to account for the random Brownian motion of both predator and prey. In our case, we are only using the less-random method of diffusion to account for the movement of the species inside Ω, our domain.

Of particular note in this oscillation of predator and prey concentrations is that any peak in the predator population happens *after* the corresponding peak in the prey population. This predator peak then causes a drop in prey concentration, which causes a drop in predator population allowing an increase in prey population and subsequent increase in predator population, and so on, producing the oscillatory effects. Absent all other factors, these oscillations will become very smooth. In reality, fluctuations in the environment cause random fluctuations in the parameters involved in the system, and thus the equilibrium population cannot attain that smooth steady state and the oscillations are essentially random fluctuations around an average value. These environmental fluctuations may be semi-cataclysmic events like earthquakes or disease, or less catastrophic events like a small change in the weather or other parameters that affect the system.

4.2 Why Stochastic Effects Matter: For Further Research

Although our model accounts for the interaction between predator and prey, by ignoring the stochastic effects of the environment, we produce a somewhat smoother distribution of species than exist in reality. The dynamics of the stochastic model allowed Liu to perturb the birth and death rates of the species as an added term to the differential equations rather than directly affecting the parameters in the deterministic model. This results in a more realistic approximation of a particular point (in space) as time passes, but does not readily allow the simulation of movement of the species through their environment.

Combining these two models into a single, coherent, *solvable* model would allow both results to be seen. That is, the effect of both environmental fluctuations and movement or migration of species could be seen at the same time. Naturally, this would make some analysis more difficult, but comparison to previous analytical and empirical results could simplify that analysis. Additionally, combining both models would allow consideration of "what-if" scenarios with more useful results.

Finally, additional comparison between the two functional responses and an approximate determination of when 3a takes over from 3b, if in fact a complete "take-over" occurs would be interesting. Additionally, we feel the need for numerics to solve these kinds of complex non-linear problems presents a unique opportunity to combine all four parts of these models into a truly solvable whole.

Appendices

A Boundary Condition Approximation

Since we want zero-flux boundary conditions, we will reflect across the boundary. We will set "ghost points" outside our boundary (e.g., $(0,-1)$ and $(-1,0)$ for the bottom-left corner of Ω) whose values will be the same as the real points inside Ω. Then using finite-difference to approximate the spatial derivative across the boundary we get zero flux. Since we are in two dimensions, we have the four sides of the square that is Ω, but the five-point stencil to approximate the LaPlacian requires a bit more work at the corners.

For the sides of the square ($1 \leq i, j \leq M-1$) we have

$$U^k_{i,-1} := U^k_{i,1} \qquad U^k_{i,M+1} := U^k_{i,M-1} \qquad U^k_{-1,j} := U^k_{1,j} \qquad U^k_{M+1,j} := U^k_{M-1,j}$$

$$V^k_{i,-1} := V^k_{i,1} \qquad V^k_{i,M+1} := V^k_{i,M-1} \qquad V^k_{-1,j} := V^k_{1,j} \qquad V^k_{M+1,j} := V^k_{M-1,j}$$

The five-point stencil in the interior of Ω is relatively straightforward. However, due to the right-angled triangulation of the square for the finite-element method from which our finite-difference scheme is derived, we will have slightly different conditions depending on which corner of Ω we are referring to. This gives us the following set of corner boundary conditions, which as above are essentially the same for both $U \approx u$ and $V \approx v$.

$$U^k_{0,-1} = \frac{U^k_{0,0} + U_{0,1}}{2} \qquad U^k_{-1,0} = \frac{U^k_{0,0} + U^k_{1,0}}{2} \qquad \text{(Bottom-Left corner)}$$

$$U^k_{M,M+1} = \frac{U^k_{M,M} + U_{M,M-1}}{2} \qquad U^k_{M+1,M} = \frac{U^k_{M,M} + U^k_{M-1,M}}{2} \qquad \text{(Top-Right corner)}$$

$$U^k_{M,-1} = 2U^k_{M,1} - U^k_{M,0} \qquad U^k_{M+1,0} = 2U^k_{M-1,0} - U^k_{M,0} \qquad \text{(Bottom-Right corner)}$$

$$U^k_{0,M+1} = 2U^k_{0,M-1} - U^k_{0,M} \qquad U^k_{-1,M} = 2U^k_{1,M} - U^k_{0,M} \qquad \text{(Top-Left corner)}$$

B Coefficient Matrices

The coefficient matrix from our linear system (11) is comprised of the following block definitions.

$$A^{k-1} := (1-\Delta t)I + \Delta t \operatorname{diag}\left\{\left|U_0^{k-1}\right|,\ldots,\left|U_P^{k-1}\right|\right\} + \Delta t\, L$$
$$B^{k-1} := \Delta t \operatorname{diag}\left\{\widehat{h}\left(aU_0^{k-1}\right),\ldots,\widehat{h}\left(aU_P^{k-1}\right)\right\}$$
$$C^{k-1} := (1+\Delta t\, c)I - \Delta t\, b \operatorname{diag}\left\{\widehat{h}\left(aU_0^{k-1}\right),\ldots,\widehat{h}\left(aU_P^{k-1}\right)\right\} + \delta\Delta t\, L$$

where $\widehat{h}$ is the appropriate functional response (Equations 5 and 6).

Matrix L is the second difference matrix (the Laplacian) for our numerical scheme and has the following block matrix form. Each block is $(M+1)\times(M+1)$ and so L is $(M+1)^2\times(M+1)^2$.

$$L = \frac{1}{h^2}\begin{bmatrix} S & T & & & & & \\ W & X & W & & & & \\ & W & X & W & & & \\ & & \ddots & \ddots & \ddots & & \\ & & & W & X & W & \\ & & & & W & X & W \\ & & & & & Y & Z \end{bmatrix} \qquad S = \begin{bmatrix} 3 & -\frac{3}{2} & & & & & \\ -1 & 4 & -1 & & & & \\ & -1 & 4 & -1 & & & \\ & & \ddots & \ddots & \ddots & & \\ & & & -1 & 4 & -1 & \\ & & & & -1 & 4 & -1 \\ & & & & & -3 & 6 \end{bmatrix}$$

$$T = \operatorname{diag}\left\{-\frac{3}{2},-2,-2,\ldots,-2,-2,-3\right\}$$
$$W = -I$$
$$Y = \operatorname{diag}\left\{-3,-2,-2,\ldots,-2,-2,-\frac{3}{2}\right\}$$

$$X = \begin{bmatrix} 4 & -2 & & & & & \\ -1 & 4 & -1 & & & & \\ & -1 & 4 & -1 & & & \\ & & \ddots & \ddots & \ddots & & \\ & & & -1 & 4 & -1 & \\ & & & & -1 & 4 & -1 \\ & & & & & -2 & 4 \end{bmatrix} \qquad Z = \begin{bmatrix} 6 & -3 & & & & & \\ -1 & 4 & -1 & & & & \\ & -1 & 4 & -1 & & & \\ & & \ddots & \ddots & \ddots & & \\ & & & -1 & 4 & -1 & \\ & & & & -1 & 4 & -1 \\ & & & & & -\frac{3}{2} & 3 \end{bmatrix}$$

Note that X and W are exactly the five-point stencil results for the interior points in Ω, while S, T, Y, and Z are the corresponding five-point stencil results for the corners

after being modified by the boundary conditions in Appendix A. Specifically, X is the $(i-1,j),(i,j),(i+1,j)$ points (adjusted for the left and right boundaries of Ω) and W is the $(i,j-1),(i,j+1)$ points. Similarly, S and T correspond to the lower-left to lower-right corners (the bottom of Ω), and Y and Z are the upper-left to upper-right corners (the top of Ω).

C Python Script

Attached as "PredPreyHTypeII-Both.py"

References

[1] Marcus R. Garvie. "Finite-Difference Schemes for Reaction–Diffusion Equations Modeling Predator–Prey Interactions in MATLAB". In: *Bulletin of Mathematical Biology* 69.3 (2007), pp. 931–956. ISSN: 1522-9602. DOI: 10.1007/s11538-006-9062-3. URL: https://doi.org/10.1007/s11538-006-9062-3.

[2] Qun Liu et al. "Dynamics of a Stochastic Predator–Prey Model with Stage Structure for Predator and Holling Type II Functional Response". In: *Journal of Nonlinear Science* 28.3 (2018), pp. 1151–1187. ISSN: 1432-1467. DOI: 10.1007/s00332-018-9444-3. URL: https://doi.org/10.1007/s00332-018-9444-3.